Available online at www.scholarsresearchlibrary.com

Scholars Research Library

Archives of Physics Research, 2012, 3 (3):245-257
(http://scholarsresearchlibrary.com/archive.html)

Archives of Physics Research
Scholars Research Library
ISSN : 0976-0970
CODEN (USA): APRRC7

XPS characterization and opto structural study of chemically deposited Sb (III) doped $Bi_2(Te_{1-x}Se_x)_3$ thin films

S. M. Patil[1*], S. N.Gavale[2], R.K. Mane[2], N. S. Patil[2], S. S. Mali[3], P. S. Patil[3] and P. N. Bhosale[2]

[1]D. Anandrao B. Naik College, Chikhali, Tal.- Shirala, Dist.- Sangali-415404.
[2]Materials Research Laboratory, Department of Chemistry,
Shivaji University, Kolhapur-416 004
[3] Thin Film Materials Laboratory, Department of Physics, Shivaji University, Kolhapur-416004,

---

ABSTRACT

Nanocrystalline Sb (III) doped bismuth tellurium selenide [Composition : Bi_{2-x} $Sb_x(Te_{1-x}Se_x)_3$] thin films were successfully deposited in aqueous medium by newly developed Arrested Precipitation Technique (APT) at low temperature. These thin films were prepared using a complexing agent triethanolamine (TEA) and a reducing agent sodium sulphite to avoid hydroxide formation of bismuth precursor Bi $(NO_3)_3$ and antimony precursor $(SbCl_3)$ in aqueous medium to favor the reaction with Te^{2-} and Se^{2-} chalcogen ions. The preparative conditions such as P^H, concentration of precursors, temperature, rate of agitation and time were finalized at initial stages of deposition. As deposited films were annealed at constant temperature (373K) in muffle furnace and then characterized for optostructural, morphological and compositional properties. The results demonstrate that the Bi_{2-x} $Sb_x(Te_{1-x}Se_x)_3$ thin films prepared by APT shows band gap in the range 1.46eV to 1.89eV. X-Ray Diffraction (XRD) pattern, Scanning Electron Microscopy (SEM) and Atomic Force Microscopy (AFM) images reveals that Bi_{2-x} $Sb_x(Te_{1-x}Se_x)_3$ mixed metal chalcogenide films are of nanocrystalline nature and have rhombohedral structure and better morphology. EDAX and XPS study shows good stoichiometry. Hence APT is simple and suitable for deposition of Sb (III) doped bismuth tellurium selenide thin films.

Keywords: APT, Metal chalcogenides, X-ray diffraction, XPS, AFM.

INTRODUCTION

In recent years, considerable attention has also been devoted to Sb_2Te_3, Bi_2Te_3, Bi_2Se_3, Sb_2Se_3 and multicomponent solid solutions based on bismuth and antimony chalcogenides $(Bi,Sb)_2(Te,Se,)_3$ with atomic substitutions (Sb ,Se) in the cation and anion sublattices of Bi_2Te_3 because they have been established as low-temperature thermoelectric material, and are widely employed in thermoelectric generators and coolers[1-2]. These materials also have potential applications in the fabrication of thermoelectric devices based on the Seebeck effect, such as thermal sensors, hyper frequency power sensors, thermopiles, and wide-band radiation detectors. They possess a high figure of merit Z due to a high Seebeck coefficient S, moderate electric conductivity σ, and low thermal conductivity.

Various methods of preparations of mixed Sb_2Te_3, Bi_2Te_3, Bi_2Se_3, Sb_2Se_3 thin films have been reported such as solvothermal [3], Electrodeposition [4], The pulsed magnetron sputtering [5], and also alloys of V-VI group reported by Lukyanova and Kutasov [6-8] etc reported hot extruded $(Bi,Sb)_2(Te,Se)_3$ alloys for advanced thermoelectric modules. Further these are prepared by ion beam sputtering [9], Sceen printing [10] and Thermal vacuum evaporation [11]. Many researchers working on binary, ternary and quaternary semiconducting compounds of V and VI group elements, particularly chalcogenides of bismuth, antimony and arsenic. Hence in the present investigation

Sb is doped in the ternary $Bi_2(Te_{1-x}\ Se_x)_3$ thin films by arrested precipitation technique (APT) and effects are studied [12,13].

MATERIALS AND METHODS

2. Experimental

2. 1. Preparation of Sb (III) doped $Bi_2\ (Te_{1-x}Se_x)_3$ thin films

Sb (III) doped $Bi_2\ (Te_{1-x}Se_x)_3$ mixed metal chalcogenide thin films were prepared by keeping constant amount of the 15 ml sodium tellurium sulphite, 15 ml sodium seleno sulphite (Na_2SeSO_3) for the sources of Te^{2-}, Se^{2-} respectively. Concentrations of Bi-TEA complex and Sb-TEA complex were varied in a volume stoichiometric ratio so as to obtain various compositions of Sb (III) doped $Bi_2\ (Te_{1-x}Se_x)_3$ thin films**.** Deposition of mixed Sb (III) doped $Bi_2\ (Te_{1-x}Se_x)_3$ mixed metal chalcogenide thin films was carried out by keeping all the parameters similar to those finalized for the $Bi_2\ (Te_{1-x}Se_x)_3$ thin films. Table 1. shows film composition, the variations of Bi^{3+},Sb^{3+}, Te^{2-} and Se^{2-} in Sb (III) doped $Bi_2\ (Te_{1-x}Se_x)_3$, their nomenclature, bath composition. Preparative conditions for the Sb (III) doped $Bi_2\ (Te_{1-x}Se_x)_3$ thin films are pH= 10.5 ± 0.3,Temperature= 55 ± 0.5 ^{0}C, Deposition time = 2 hrs, Substrate rotation = 45 ± 5 rpm. Thickness of the film is in between 0.19 μm to 0.80 μm

Table 1. Composition of the sample for deposition of Sb (III) doped $Bi_2\ (Te_{1-x}Se_x)_3$ thin films

Sample No.	Composition	Bath composition
D_1	$Bi_{1.98}Sb_{0.02}(Te_{0.5}Se_{0.5})_3$	(20 –x) ml 0.05 M Bi-TEA + x ml0.05 M Sb-TEA + 15 ml 0.05 M Na2TeSO3 +15ml 0.05M Na2SeSO3 and rest is water to make 100 ml total volume. x is varied from 0.0 to 0.1 ml
D_2	$Bi_{1.96}Sb_{0.04}(Te_{0.5}Se_{0.5})_3$	
D_3	$Bi_{1.94}Sb_{0.06}(Te_{0.5}Se_{0.5})_3$	
D_4	$Bi_{1.92}Sb_{0.08}(Te_{0.5}Se_{0.5})_3$	
D_5	$Bi_{1.90}Sb_{0.1}(Te_{0.5}Se_{0.5})_3$	

2. 2. Growth mechanism of $Bi_2\ (Te_{1-x}\ Se_x)_3$ thin film formation

Arrested precipitation technique is suitable for the deposition of Sb (III) doped $Bi_2\ (Te_{1-x}Se_x)_3$ mixed type thin films. In the present investigation, we have slightly modified the chemical deposition method using polydentate chelating agent such as triethanolamine [N $(CH_2\text{-}CH_2\text{-}OH)_3$] as a complexing agent to arrest Bi^{3+} and Sb^{3+} ions. Organic complexing agent TEA have strong affinity towards the Bi^{3+} and Sb^{3+} ions and it's tendency to keep the Bi^{3+} and Sb^{3+} ion arrested in a solution even in alkaline pH range where the metal hydroxide formation is possible. Here ionic species of $Bi^{3+,}$ Sb^{3+}, $Te^{2-}$and Se^{2-} are produced as per the following reaction equilibria.

Bi^{3+}, Sb^{3+}, Te^{2-} and Se^{2-} ions are slowly releases in the solution in an aqueous alkaline medium deposition of Sb(III) doped $Bi_2(Te_{1-x}Se_x)_3$ is takes place. The formation of Sb (III) doped $Bi_2\ (Te_{1-x}Se_x)_3$ thin films occurs when ionic product of Bi^{3+}, Sb^{3+}, Te^{2-} and Se^{2-} exceeds the solubility product of Sb (III) doped $Bi_2\ (Te_{1-x}Se_x)_3$. Overall growth mechanism of the mixed composites of bismuth antimony tellurium selenide is summarized as follows.

$(NH_4)_3[Bi_2\ N\ (CH_2\text{-}CH_2\text{-}O)_3] + 6H_2O \rightarrow Bi^{3+} + 3NH_4OH + 3OH^- + 2[N(CH_2\text{-}CH_2\text{-}OH)_3]$ (1)

$(NH_4)_3[Sb_2\ N\ (CH_2\text{-}CH_2\text{-}O)_3] + 6H_2O \rightarrow Sb^{3+} + 3NH_4OH + 3OH^- + 2[N(CH_2\text{-}CH_2\text{-}OH)_3]$ (2)

$Na_2TeSO_3 + OH^- \rightarrow Na_2SO_4 + HTe^-$ (3)

$HTe^- + OH^- \rightarrow H_2O + Te^{2-}$ (4)

$Na_2SeSO_3 + OH^- \rightarrow Na_2SO_4 + HSe^-$ (5)

$HSe^- + OH^- \rightarrow H_2O + Se^{2-}$ (6)

The reactions given in equation (1) to (6) shows that the Bi^{3+}, Sb^{3+}, Te^{2-} and Se^{2-} are condenses ion by ion basis on the glass substrate at pH 10.5 and 55^{o}C temperature as follows:

$Bi^{3+} + Sb^{3+} nNa_2TeSO_3 + nNa_2SeSO_3 \rightarrow Bi_{2-x}Sb_x(Te_{1-x}\ Se_x)_3 + nNa_2SO_4 + n(TEA)$ (7)

Finally, the deposited Sb (III) doped $Bi_2\ (Te_{1-x}Se_x)_3$ films prepared by arrested precipitation technique are found to be uniform and well adherent to the substrate.

RESULTS AND DISCUSSION

3. 1 X-ray Diffraction (XRD) Study

X- ray diffraction (XRD) analysis was carried out for all samples using a Philips PW-1710 X-ray diffractometer for the 2θ ranging from 10^0 to 100^0 with Cr K_α line used as a beam (λ=2.25 A^0). XRD pattern of the doped thin films are shown in Figure 1 From the XRD pattern it is seen that thin film shows nanocrystalline nature. All Sb (III) doped $Bi_2(Te_{1-x}Se_x)_3$ shows a rhombohedral structure. The comparison of the observed'd' values and the crystallite size of the film calculated using Debye Scherrer formula of the deposited samples are given in Table 2.

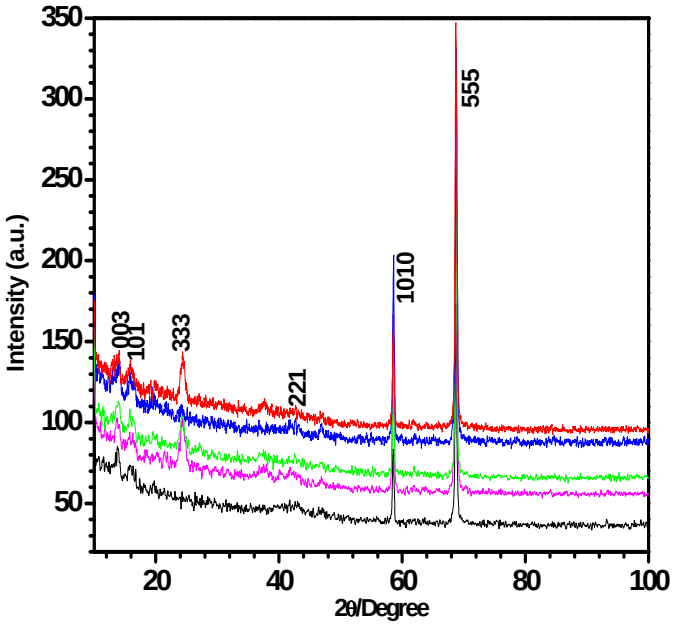

Figure 1 XRD pattern of Sb (III) doped $Bi_2(Te_{1-x}Se_x)_3$thin films.

Doped thin films having different composition (x =0.2 to 0.1 ml) deposited at 55 ^oC. The presence of most intense diffraction peaks at (555), (1010), (003), (101), (333) and (221) were found. The plane indices are obtained by comparing the intensities and positions of the peaks with those of Bi_2Se_3, Bi_2Te_3, Sb_2Se_3 and Sb_2Te_3, which are given by JCPDS file no.85-0519, 85-0439, 75-1462, 72-1990, etc.

Table 2. XRD results of the Sb (III) doped $Bi_2(Te_{1-x}Se_x)_3$ thin films for various compositions

Film Composition	Observed 'd' value (A^o)	JCPDS 'd' values A^o		Crystallite size 'D' (nm)
		'd'(A)	(hkl)	
$D_1=Bi_{1.98}Sb_{.02}(Te_{0.5}\ Se_{0.5})$	9.44	9.43	003	42.13
	5.40	8.02	333	
	2.34	2.34	343	
	2.02	2.02	413	
	1.57	1.58	224	
$D_2=Bi_{1.96}Sb_{.04}(Te_{0.5}\ Se_{0.5})$	9.96	9.96	003	41.67
	8.28	5.07	101	
	5.07	2.41	201	
	2.34	2.34	101	
	2.02	2.02	503	
$D_3=Bi_{1.94}Sb_{.06}(Te_{0.5}\ Se_{0.5})$	9.50	9.96	003	39.89
	5.45	5.07	335	
	2.87	2.87	221	
	2.34	2.34	403	
	2.16	2.16	205	
	2.10	2.07	343	
	2.02	2.02	413	
$D_4=Bi_{1.92}Sb_{.08}(Te_{0.5}\ Se_{0.5})$	8.28	9.96	101	39.38
	5.47	5.07	222	
	3.52	3.58	012	
	3.14	3.13	015	
	2.88	2.89	221	
	2.33	2.33	304	
	2.21	2.23	443	
	2.02	2.02	413	
	1.80	1.80	131	
$D_5=Bi_{1.90}Sb_{.1}(Te_{0.5}\ Se_{0.5})$	9.40	8.28	003	39.36
	5.43	5.07	222	
	2.34	3.58	403	
	2.02	3.13	555	
	1.57	2.89	0210	

The strongest peak for all films occurred at 2θ = 68.78° with d = 2.02A°. From the crystalline size (D) of the deposited thin films it reveals that intensity of the peak decreases with doping of Sb (III) and broadening of small peaks. This attributed to the fact that there might be decrease in crystallite size on Sb (III doping in $Bi_2(Te_{1-x}\ Se_x)_3$ thin films; also small degree of broadening occurs as a result of increase in strain in the film due to Sb incorporation in the Bi lattice site. Careful observation of the XRD pattern of the films shows that some peaks are remained unchanged and some new lines appeared in the pattern. The increase in the number of new peaks are due to introduction of new planes because of Sb(III), caused by non uniform distortion as a result of doping [10].

3. 2 UV-Visible spectroscopic Study

The optical absorption coefficient (α) of Sb (III) doped $Bi_2(Te_{1-x}Se_x)_3$ is found to be in the order of 10^5 cm^{-1}. The dependence of the optical absorption on the photon energy is described by the relation,

$$\alpha = \frac{A}{h\nu}(h\nu - Eg)^n \quad \text{.....8}$$

$(\alpha h\nu)^2$ vs hν for Sb (III) doped $Bi_2(Te_{1-x}Se_x)$ having different composition was plotted and the values of the optical band gap E_g were taken as the intercept of $(\alpha h\nu)^2$ vs hν on energy axis at α=0 as shown in Figure 2. The estimated values of E_g of different composition of Sb (III) doped $Bi_2(Te_{1-x}Se_x)_3$ films are listed in Table 3 The substitution of 'Sb' atoms by 'Bi' atoms in $Bi_2(Te_{1-x}Se_x)_3$ thin films results in increasing the optical band gap of the system. The increasing in band gap is caused by alloying effect. This effect causes changes in bond angles and/or bond lengths. The same observation was found by M. M. El-Samanoudy for replacement of Sb atoms by Bi atoms in case of $Ge_{25}Sb_{15-x}Bi_xS_{60}$ thin films [14]. From Figure 2 the type of transition is direct and allowed. It was found that the optical energy gap E_g increases gradually from 1.46 eV to 1.89 eV with increasing Sb in 0.02 % to 0.1 %. SEM micrograph shows decrease in grain size which is evidence for the increase of band gap with Sb doping concentration. Another reason is antimony atoms (1.33 A^0) are smaller than bismuth atoms (1.43 A^0) and possess lower-energy atomic orbital, which can lead to wider energy gap by lowering top of the valence band and more importantly raising the bottom of the conduction band. Also vary small grain size (nanometer size) could shift the band gap to higher values compared with the bulk crystalline value [15]

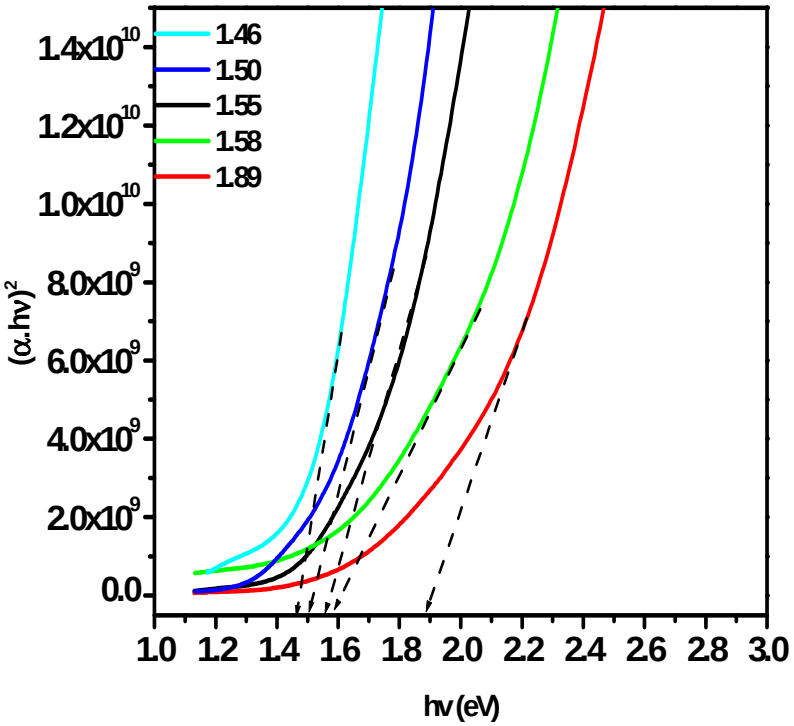

Figure 2 Plot of $(\alpha h\nu)^2$ vs hν for Sb (III) doped $Bi_2(Te_{1-x}Se_x)_3$ thin films

Table 3. Variation of band gap for Sb (III) doped $Bi_2(Te_{1-x}Se_x)_3$ thin films

Film composition	Band Gap (Eg) eV
$D_1 = Bi_{1.98}Sb_{0.02}(Te_{0.5}Se_{0.5})_3$	1.46
$D_2 = Bi_{1.96}Sb_{0.04}(Te_{0.5}Se_{0.5})_3$	1.50
$D_3 = Bi_{1.94}Sb_{0.06}(Te_{0.5}Se_{0.5})_3$	1.55
$D_4 = Bi_{1.92}Sb_{0.08}(Te_{0.5}Se_{0.5})_3$	1.58
$D_5 = Bi_{1.90}Sb_{0.1}(Te_{0.5}Se_{0.5})_3$	1.89

3. 3 Scanning Electron Microscopic (SEM) Study

Scanning electron micrograph of Sb (III) doped $Bi_2(Te_{1-x}Se_x)_3$ at 10000 X magnification is shown in Figure 3 The SEM micrographs shows well adherent, smooth and uniform film surface without cracks under low magnification which accounts high mechanical stability of the samples. We have observed significant variation in the morphological properties of the films for the variation of Sb doping.

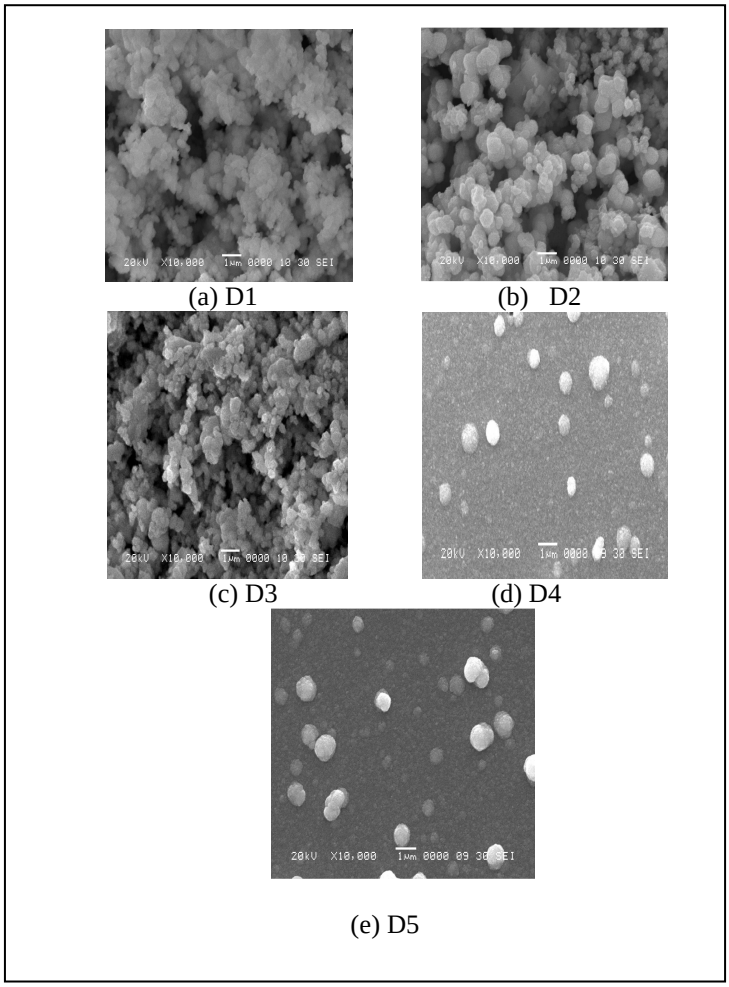

Figure 3 SEM micrographs for Sb (III) doped $Bi_2(Te_{1-x}Se_x)_3$ thin films.

After doping Sb(III) slightly cross linked grains coalesce and aggregates of crystallites are formed .In some regions overgrowth were also observed. It shows the co-existence of small and relatively large grains on the film surface. Figure 3 $D_1$to D_5 shows that large crystallites are broken to well define nanocrystalline particles with fine background as a result of further antimony (III) doping. These micrographs reveal that the grain size decreases, as the concentration of doping of Sb (III) increases. The result of increase in Sb doping indicating that Sb is grain growth inhibitor in $Bi_2(Te_{1-x}Se_x)_3$ films. Grain size was determined using the linear intercept technique.

The grain size of the antimony (III) doped Bi_2 $(Te_{0.5}Se_{0.5})_3$ thin films with x= 0.02, 0.04, 0.06, 0.1 are 650 nm, 548nm, 398nm 267nm and 140 nm respectively. These results are consistent with the XRD results which also show broadening of peaks as a result of antimony (III) doping indicating decrease of crystalline size [16].

3. 4 Energy Dispersive X-ray Analysis (EDAX)

Compositional analysis of Sb (III) doped $Bi_2(Te_{1-x}Se_x)_3$ thin films was carried out by EDAX analysis. EDAX Images of few samples are shown in Figure 4.

The doping (Sb) concentration in the starting solution was varied from 0.02% to 0.1%. The atomic percentage ratio of Bi, Sb, Te and Se in deposited thin films is listed in Table 4, it shows that the samples are in good stoichiometric ratio. Deviation from the atomic percentage of Bi, Sb, Se, and Te in Sb (III) doped $Bi_2(Te_{1-x}Se_x)_3$ could be attributed due to the presence of oxygen. Oxygen may be incorporated into the film either from the atmosphere or from the alkaline medium of the bath solution. In our chemical bath deposition experiment, the p^H is maintained in alkaline condition and hence there is significant influence of OH^- ions on the deposition process, which favors the inclusion of oxygen in the deposited films, resulting in oxygen contamination. The excess of Sb bounded to oxygen and hydrogen in the form of $Sb(OH)_3$ and Sb_2O_3. Same type of conclusion was observed in XPS analysis [10]

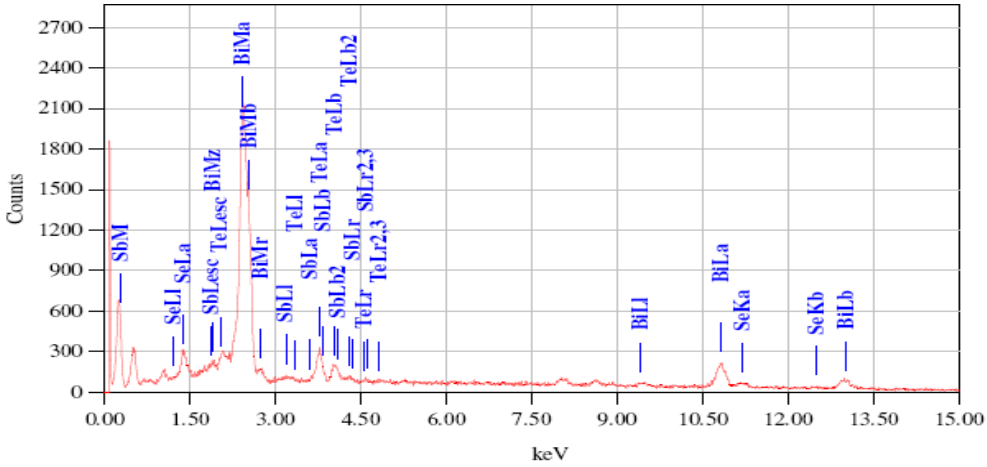

a) ***$D_1=Bi_{1.98}Sb_{0.02}(Te_{0.5}Se_{0.5})_3$***

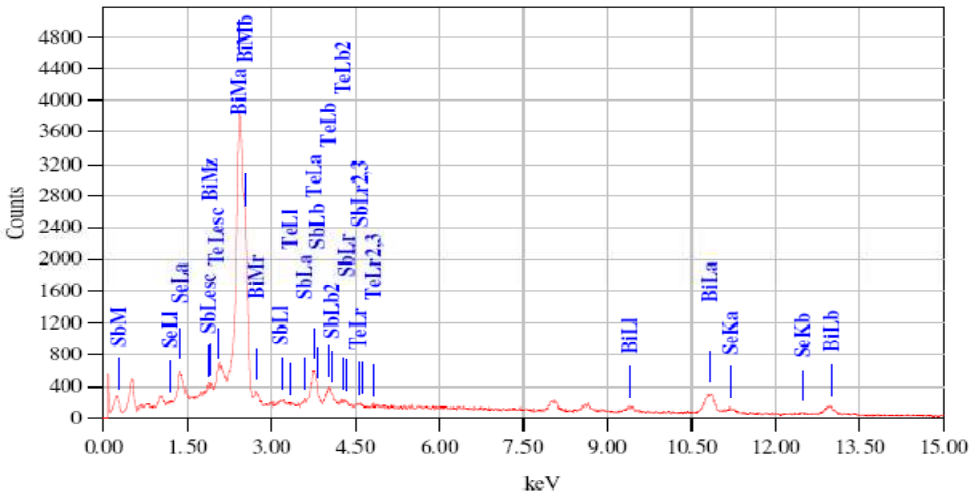

b) $D_3=Bi_{1.94}Sb_{0.06}(Te_{0.5}Se_{0.5})_3$

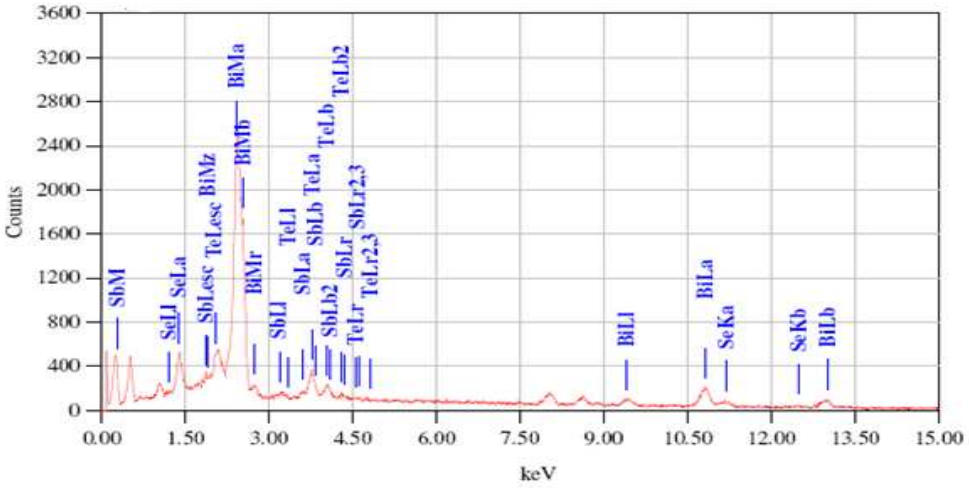

c) D_5= $Bi_{1.90}Sb_{0.1}$ $(Te_{0.5}Se_{0.5})_3$

Figure 4 EDAX spectra of Sb (III) doped $Bi_2(Te_{1-x}Se_x)_3$ thin films

Table 4. Quantitative analysis of Bi, Sb,Te and Se by using EDAX for Sb (III) doped $Bi_2(Te_{1-x}Se_x)_3$

Film composition	Elements	Atomic percentage	
		Observed	Expected
D_1 $Bi_{1.98}Sb_{0.02}(Te_{0.5}Se_{0.5})_3$	Bi	43.42	39.60
	Sb	0.45	0.40
	Te	26.85	30.00
	Se	29.28	30.00
D_2 $Bi_{1.96}Sb_{0.04}(Te_{0.5}Se_{0.5})_3$	Bi	44.48	39.20
	Sb	0.89	0.80
	Te	26.70	30.00
	Se	27.93	30.00
D_3 $Bi_{1.94}Sb_{0.06}(Te_{0.5}Se_{0.5})_3$	Bi	44.95	38.80
	Sb	1.28	1.20
	Te	27.00	30.00
	Se	26.77	30.00
D_4 $Bi_{1.92}Sb_{0.08}(Te_{0.5}Se_{0.5})_3$	Bi	43.75	38.40
	Sb	1.66	1.60
	Te	27.50	30.00
	Se	27.09	30.00
D_5 $Bi_{1.90}Sb_{0.10}(TSe_{0.5}Se_{0.5})_3$	Bi	42.98	38.20
	Sb	1.90	1.80
	Te	26.95	30.00
	Se	28.25	30.00

3. 5 Atomic Force Microscopy (AFM) Study

A quantitative method to examine the surface morphology and structure is obtained by analyzing the surface roughness using AFM. The surface roughness can be given with a statistical parameter- root mean square (rms or Rq)

Atomic Force Microscopy (AFM) was performed on a JEOL-JSM- microscope. Analysis of Sb (III) doped $Bi_2(Te_{1-x}Se_x)_3$ thin films deposited by arrested precipitation technique was done by AFM analysis. Figure 5 shows that 2D and 3D AFM images for D_1 to D_5 samples. In 3D image, intensity strip indicates the height of the surface grains along z-axis. AFM study reveals that, granular nature of the particles [17]. It was observed that the surface roughness of the film decreases from 11.5, 9.69, 8.15, 7.39 and 5.58. nm/1μm^3 for D_1 to D_5 sample respectively. From the AFM images it was observed that the AFM images are in well agreement with the SEM images and it reveals a low level of roughness.

3. 6 X-ray Photoelectron Spectroscopic (XPS) Study

Binding energy, elemental composition and surface nature of antimony (III) doped $Bi_2(Te_{0.5}\ Se_{0.5})_3$ was confirmed by using X-ray photoelectron spectroscopy (XPS). The XPS data were collected in the constant analyzer energy mode at 20 eV. Mg Kα (hν = 1253.6 eV) radiation was employed as the excitation source with an anode voltage of 15 kV and an emission current of 20 mA. Figure 6 shows a survey spectrum of the Sb (III) doped $Bi_2(Te_{1-x}Se_x)_3$ thin

film [Only D_3sample]. The XPS survey scan of the Sb (III) doped $Bi_2(Te_{1-x}Se_x)_3$ reveals C, Bi, Sb,Te, Se and O peaks obtained using C1s as the reference at 285 eV. It indicates that the binding energies of different states of the elements present in the films are 170.5, 529, 582.2 and 55.03 eV for Bi, Sb Te, and Se respectively.

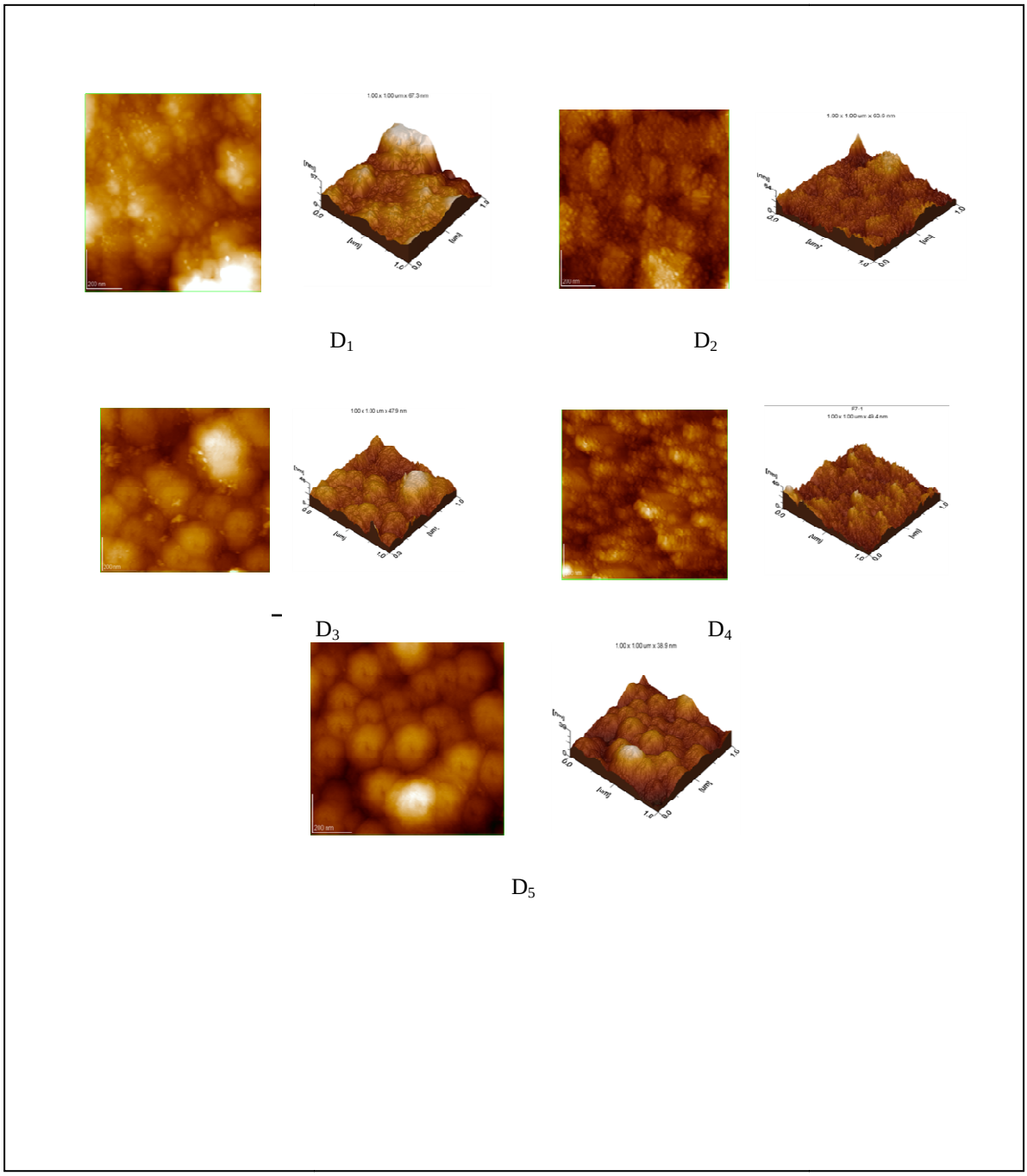

Figure 5. 2D and 3D AFM images of Sb (III) doped $Bi_2(Te_{1-x}Se_x)_3$thin films

The presence of the O 1s peak at 529 eV indicates that oxidation of the film may be takes place due to exposure to the atmosphere. The high-resolution spectrum of Sb(III) in (Figure 6.5 c) shows a peak for $Sb_{3d5/2}$ and $Sb_{3d3/2}$ peaks are observed at 529.7 and 537.3 eV, respectively. A broad peak for Sb $_{3d5/2}$ is obtained due to overlapping with the O 1s (529.6 eV) peak, because the presences of O1s and Sb3d3/2 peaks are present at same binding energy at 529 eV. The peak at 529.eV is due to $Sb_{3d3/2}$ this is confirmed by EDAX result, so the Sb $3d_{3/2}$ peak is more suitable than the Sb $3d_{5/2}$ peak for quantification [18]. The Bi $4f_{5/2}$ and $4f_{7/2}$ peaks are found at the 159 eV corresponds to $Bi_{1.94}Sb_{0.06}(Te_{0.5}\ Se_{0.5})_3$ consistent with the phase identified by XRD. These peaks are supported by the presence of Te 3d state at 582.2 eV as shown in Figure 7 (d) [19]. The Te $3d_{5/2}$ and $3d_{3/2}$ peaks were located at 572.0 and 582.3

eV respectively. This analysis of sample is consistent with the XRD data. After the initial oxidation, the surface oxide layer acts as a protective layer preventing further oxidation.

The quantification in XPS is determined by considering the intensity of photoelectron spectra by equation

$$I = J\rho\sigma K\lambda \qquad 9$$

where J is the photon flux, ρ is the concentration of the atom or ion in the solid, σ is the cross-section for photoelectron production (which depends on the element and energy being considered), K is a term which covers all of the instrumental factor (0.7 for MgKλ), and λ is the electron attenuation length. The intensity referred to will usually be taken as the integrated area under the peak following the subtraction of a linear or S-shaped background. The above equation was used for direct quantification and summarized in Table 5. Stoichiometries of as deposited films by APT technique were determined by EDAX and XPS results are tabulated in Table 5. Comparative studies on chemical composition of thin films from above result shows that, bismuth, antimony, tellurium and selenium in $Bi_{1.94}Sb_{0.06}(Te_{0.5}\ Se_{0.5})_3$ thin films is made to know they are satisfactory assessed for the determination of percentage error. The amount of bismuth, antimony, tellurium and selenium found by EDAX is in agreed with results obtained by XPS analysis. Further the experimental values are well matched with theoretical initial values taken for deposition of thin films.

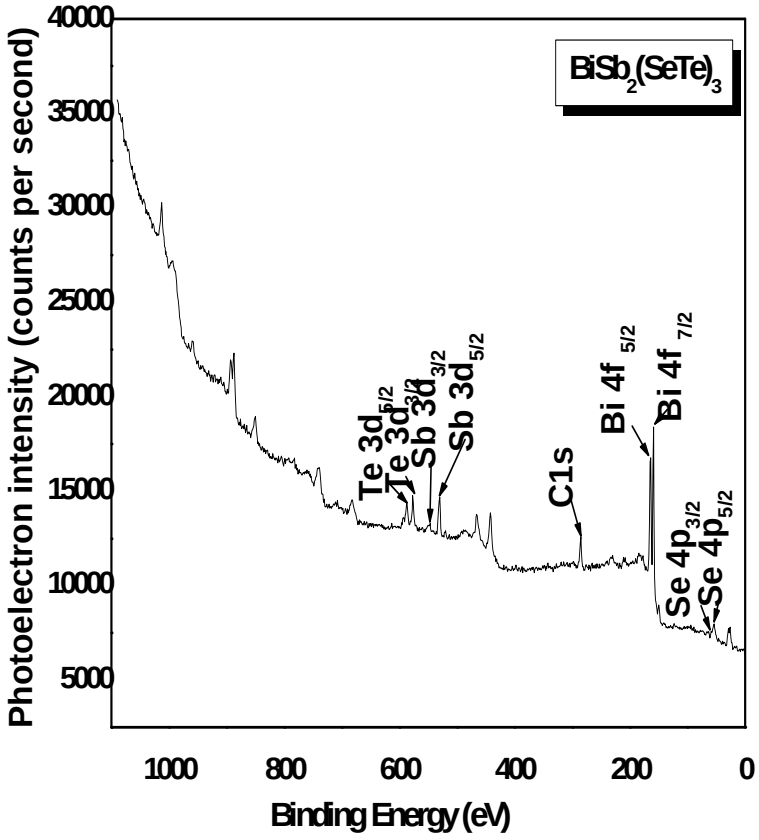

Figure 6. XPS spectrum of Sb (III) doped $Bi_2(Te_{1-x}Se_x)_3$thin film

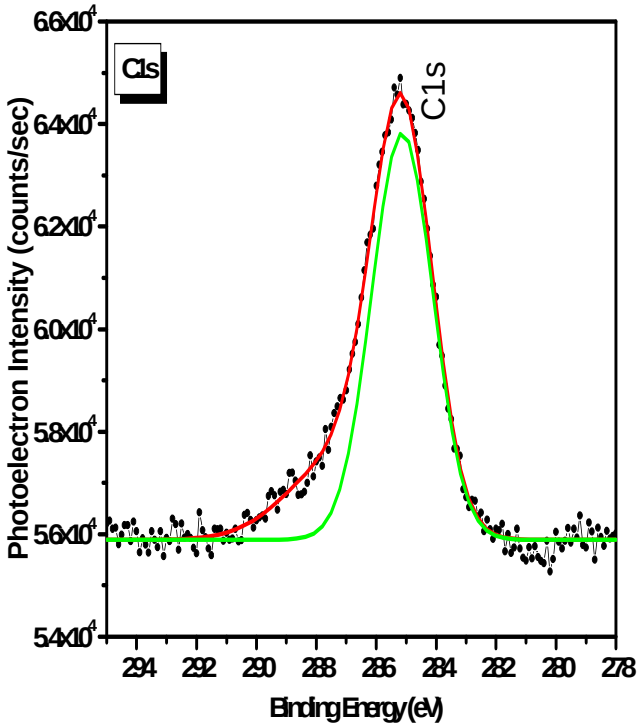
C1s
C1s
Photoelectron Intensity (counts/sec)
Binding Energy (eV)

a) **C1S**

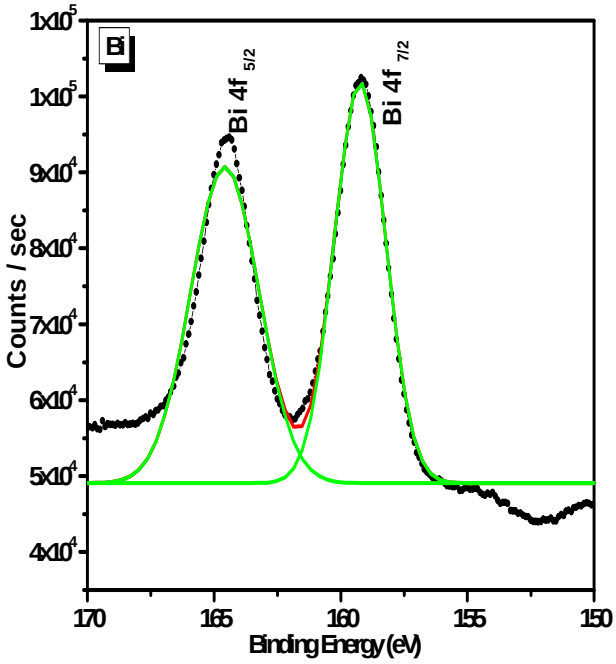
Bi
Bi 4f 5/2
Bi 4f 7/2
Counts / sec
Binding Energy (eV)

b) Bi4f

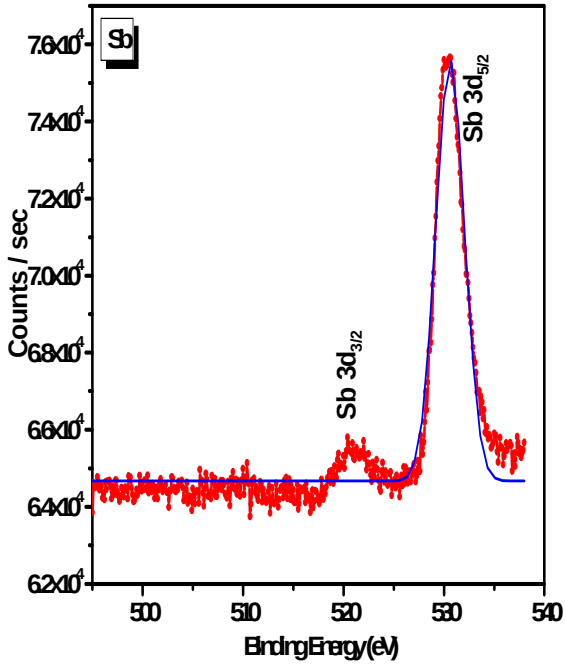
Sb
Sb 3d3/2
Sb 3d5/2
Counts / sec
Binding Energy (eV)

c) Sb3d

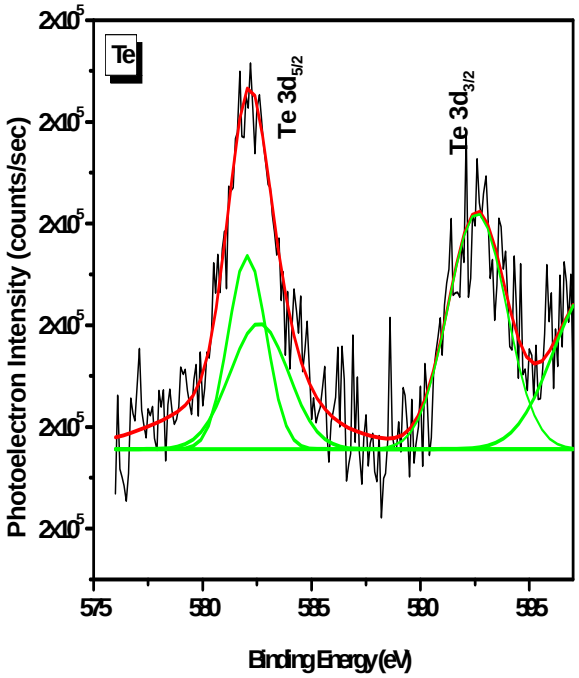
Te
Te 3d5/2
Te 3d3/2
Photoelectron Intensity (counts/sec)
Binding Energy (eV)

d) Te3d

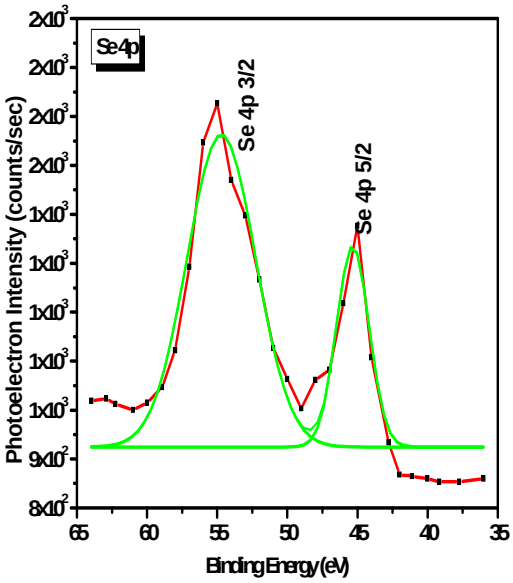

e) Se 4p

Figure 7. XPS spectra showing a) C1S, b) Bi 4f , c) Sb 3d , d) Te 3d , e) Se 4p states

Table 5 . Comparative quantitative elemental analysis of Sb (III) doped $Bi_2(Te_{1-x}Se_x)_3$.

Film Composition	Element	Elements (Expected at %)	Elements by XPS (Actual at %)	Elements by EDAX(Actual at %)
$Bi_{1.94}Sb_{0.06}(Te_{0.5}\ Se_{0.5})_3$	Bi	38.80	39.90	44.95
	Sb	1. 20	1.25	1.28
	Te	30.00	28.64	27.00
	Se	30.00	27.87	26.77

CONCLUSION

It is concluded that Sb (III) doped $Bi_2(Te_{1-x}Se_x)_3$ thin film was successfully deposited by APT and characterized for their opto structural and morphological properties. The UV-Vis spectrum of the films reveals that the deposited films having band gap in the range of 1.46 eV to 1.89 eV. The XRD of the film shows rhombohedral structure. SEM and AFM micrograph shows that films are compact, uniform and adherent with pin-hole-free nature. From EDAX the compositions of the films are in good stoichiometric ratio. Further study is going on to observe the suitability of Sb (III) doping in $Bi_2(Te_{1-x}Se_x)_3$ thin film material for photo fabrication of electrode in ECPV cell, dye sensitised ECPV cell and thermo cooling devices.

REFERENCES

[1] L. N. Lukyanova, V. A. Kutasov and P. P. Konstantinov, *Phys. Solid State*, **2008**, 50, 2237.
[2] S. V. Ovsyannikov, Yu. A. Grigor'eva, G. V. Vorontsov, L. N. Luk'yanova, V. A. Kutasov and V. V. Shchennikov, *Phys. Solid State*, **2012**, 54, 261.
[3] W. Wang, B. Poudel, J. Yang, D. Z. Wang, and Z. F. Ren, *J. Am. Chem. Soc.* , **2005**,127, 13792.
[4] D. D. Frari, S. Dilibereto, N. Stein, C. Boulanger, J. M. Lecuire, *Thin Solid Films*, **2005**, 483, 44.
[5] K. Wojciechowski, E. Godlewska, K. Mars, R. Mania, G. Karpinski, P. Ziolkowski, C. Stiewe, E. Muller, *Vacuum*, **2008**, 82, 1003.
[6] L. N. Lukyanova, V. A. Kutasov, P. P. Konstantinov, & V. V. Popov, *J. Electronic Mater*., **2010**, 39, 2070.
[7] V. A. Kutasov and L. N. Luk'yanova, Fiz. Tverd. Tela, Phys., *Solid State*, **2006**, 48, 2289.
[8] L. N. Lukyanova, V. A. Kutasov, and P. P. Konstantinov, Fiz. Tverd. Tela, *Phys. Solid State*, **2005**, 47, 233.
[9] H. Noro, K. Sato, and H. Kagechika, *J. Appl. Phys*., **1993**, 73,1252.
[10] C. Navone, M. Soulier, M. Plissonnier and A. L. Seiler, *J. Electronic Mater.*, **2010**, 39, 1755.
[11] B. S. Farag, A. M. Abou EL Soud, H. A. Zayed, S.A.Gad, *J. Ovonic Research*, **2010**, 6, 267.
[12] S. M. Patil, S. R. Mane, R. M. Mane, S. S. Mali, P. S. Patil, P. N. Bhosale, *Canadian J. Chemistry*, **2011**, 89,1375.
[13] R.M. Mane, S.R. Mane, R. R. Kharade, P.N. Bhosale, *J. Alloys Compds.*, **2010**, 491,321.
[14] M. M. El-Samanoudy, *Thin Solid films*, **2003**, 423,201.

[15] P. Lostak, C. Drasar, H. Sussmann, P. Reinshaus, R. Novotny and L. Benes, *J. Cry. Growth*, **1997**, 179,144.
[16] N. S. Patil, A. M. Sargar, S. R. Mane, P. N. Bhosale, *Appl. Surface Sci.*, **2008**, 254,5261.
[17] V. Richoux, S. Diliberto.& C. Boulanger, *Electro. Mater*., **2010**, 39, 1914.
[18] S. Shi, M. Cao, & C. Hu, *J. Crystal Growth Design*, **2009**, 9, 2057.
[19] S. S. Garje, J. D. Eisler, S. J. Ritch, M. Afzaal, Paul O'Brien, and T. Chivers, *J. Am. Chem. Soc*., **2006**, 128, 3120.